

Improvement of quantification and identification of atmospheric reactive mercury

Adriel Luippold^a, Mae Sexauer Gustin^{a,*}, Sarah M. Dunham-Cheatham^a, Lei Zhang^b

^a Department of Natural Resources and Environmental Science, University of Nevada-Reno, Reno, NV, USA, 89557

^b School of the Environment, Nanjing University, Nanjing, Jiangsu, 210023, China

HIGHLIGHTS

- The Hg community needs a method that allows for better measurement of RM = GOM+PBM.
- A method was improved to quantify RM compounds and chemistry.
- A statistical method was developed that allowed for quantifying RM compounds.
- Sample replication was improved, as was resolution of RM quantification and speciation.
- The UNR-RMAS 2.0 is a viable method for quantifying RM concentrations and chemistry.

ARTICLE INFO

Keywords:

GOM
Thermal desorption
UNR-RMAS
Pyrolyzer
Cation exchange membrane

ABSTRACT

The mercury (Hg) research community is in need of a method to quantify reactive, gaseous oxidized, and particulate-bound Hg compounds. The University of Nevada, Reno-Reactive Mercury Active System (UNR-RMAS) was designed to quantify reactive Hg, as well as identify compounds present in the atmosphere. This system has undergone significant improvements and is now designated as UNR-RMAS 2.0. The system physical design, flow management, and sample analytical methods have been improved. A new sample manifold increased reliability and consistency of air flow. The thermal desorption method for identification of gaseous oxidized Hg compounds was improved with respect to temporal resolution and temperature management. A statistical method was developed that allows for quantifying reactive Hg (RM) compounds. In addition, analyses of anions on nylon membranes was investigated as means of understanding air mass chemistry and potential RM compounds. The results of these improvements are demonstrated through comparison of a year of UNR-RMAS 2.0 sample data collected in 2018–2019 with that collected in 2014–2015. Implemented changes resulted in improved sample replication and resolution of RM quantification and speciation.

1. Introduction

There is a demonstrated need for a mercury (Hg) measurement system that allows for quantification of gaseous oxidized Hg (GOM), particulate-bound Hg (PBM), and reactive Hg (RM = GOM + PBM). The only commercially available system for measurement of atmospheric Hg is the Tekran® 2537/1130/1135 (Tekran® Corporation, Toronto, Canada) system designed to quantify GEM, GOM, and PBM, respectively. Studies have shown the Tekran® system underestimates the amount of GOM in the air (Ariya et al., 2015; Gustin et al., 2015), and there are demonstrated interferences associated with the GOM measurement (Gustin et al., 2013; Lyman et al., 2010; Maruszczak et al., 2017; McClure

et al., 2014), and artefacts associated with the PBM measurement (Talbot et al., 2011). Results of the Reno Atmospheric Mercury Inter-comparison eXperiment (RAMIX) indicated that GOM not collected by the denuder was collected by the 1135 PBM unit (Gustin et al., 2013). In addition, it is important to understand the chemistry of RM, GOM, and PBM. This is necessary to determine deposition velocities and potential impacts to ecosystems and humans. The University of Nevada, Reno-Reactive Mercury Active System (UNR-RMAS) is an active sampling system with cation exchange and nylon membranes used as collection surfaces for RM (Huang et al., 2013, 2017; Pierce and Gustin, 2017). Cation exchange membranes (CEM) provide a quantitative measurement of RM, and nylon membranes provide a collection surface

* Corresponding author.

E-mail address: mgustin@cabnr.unr.edu (M.S. Gustin).

<https://doi.org/10.1016/j.atmosenv.2020.117307>

Received 9 November 2019; Received in revised form 31 December 2019; Accepted 25 January 2020

Available online 28 January 2020

1352-2310/© 2020 Elsevier Ltd. All rights reserved.

that is thermally desorbed allowing for identification of RM compounds (Gustin et al., 2013, 2016; Huang and Gustin, 2015a, 2015b; Huang et al., 2013, 2017). The UNR-RMAS reported in previous studies (Gustin et al., 2016; Huang et al., 2013) has been significantly changed to improve sampling resolution (1-week instead of 2-week sampling period) and analytical methods. The improved system is designated as the UNR-RMAS 2.0. This paper discusses the modifications made to the system and compares data collected with the UNR-RMAS 2.0 to data collected with the UNR-RMAS and Tekran® systems. A Tekran® 2537/1130 system and UNR-RMAS 2.0 were deployed next to each other at the University of Nevada, Reno's College of Agriculture, Biotechnology, and Natural Resources Valley Road Greenhouse Facility in Reno, Nevada, USA (1377 m asl, 39° 32' 14.87" N, 119° 48' 16.93" W) from March 2018 to March 2019. Our objectives were to refine the UNR-RMAS system and improve analytical methods. It was hypothesized that the UNR-RMAS 2.0 would collect Hg more efficiently than the Tekran® system based on the performance of the UNR-RMAS, and that replication and resolution would improve with the modifications made to the thermal desorption method. An additional limitation of the UNR-RMAS is that the method for determining RM chemistry was qualitative. Here, a more quantitative method was developed. This is a first step for quantifying the amount of different RM compounds.

2. Materials and methods

2.1. General principles

The first UNR-RMAS design, as discussed in Huang et al. (2013), utilized 6 vacuum pumps to pull air at an approximate standard flow rate of 1 L per minute (Lpm; 1 atm, 0 °C) through 1 sample line each. On each sample line, 2 consecutive single-stage filter holders containing an upstream (termed "A" membrane) and downstream (termed "B" membrane) CEM or nylon membrane collected RM. The downstream membrane was used to capture breakthrough Hg that passed through the upstream membrane. Due to issues with the vacuum pumps the system was modified such that flow rate was controlled by Teflon valves that were manually adjusted to 1 Lpm by operators or controlled using mass flow controllers. Pumps and flow control valves had to be placed indoors to minimize weather damage, while the collection manifold was outside. The apparatus holding the filters in place was made of plastic and degraded quickly due to weather exposure (Huang et al., 2013). The updated sample manifold is displayed in Supporting Information (SI) Fig. SI 1. Upstream nylon membranes were analyzed using a custom-built thermal desorption system (Huang et al., 2013). Upstream and downstream CEM and downstream nylon membranes were analyzed using cold vapor atomic fluorescence spectroscopy (CVAFS, Tekran® 2600 following EPA method 1631E(2002)).

Many steps of the deployment procedures for the UNR-RMAS and the UNR-RMAS 2.0 are similar, including: 1) new membranes are loaded into filter holders that are tightened with plastic wrenches creating an air-tight seal, and the filter holders are promptly connected to the sample manifold; 2) pumps are switched on and the flow rate through each filter is measured; 3) at the end of deployment, flow rates through filters are measured and the pumps turned off; and 4) filter holders are removed from the manifold to a clean area where membranes are transferred to storage containers using clean Teflon® tape-wrapped tweezers for storage. Three sample membrane blanks are collected at the same time as sample collection with Teflon® wrapped tweezers (newly wrapped each collection) and placed in storage containers; these blanks are analyzed to determine how much Hg is contained on the sample membranes prior to deployment. Sample and blank membranes are stored at -20 °C until analyzed by thermal desorption for upstream nylon membranes or a Tekran® 2600 for CEM and downstream nylon membranes, respectively.

2.2. Membranes

For both UNR-RMAS and UNR-RMAS 2.0, RM was collected on two membrane types, CEM and nylon membranes. For each deployment period, three upstream and downstream sample membranes of each filter type were deployed. It has been demonstrated using a polytetrafluoroethylene (PTFE) membrane to separate PBM and GOM that the membranes in Reno, NV that PBM made up 22–52% RM (Gustin et al., 2019). Given the study design, Hg collected on the membranes in this study is referred to as RM (Gustin et al., 2013).

The CEM material is a negatively charged polyethersulfone membrane (0.8 µm pore size; Mustang-S, Pall Corporation). CEM have been widely applied for RM measurements in ambient air (Caldwell et al., 2006; Castro et al., 2012; Ebinghaus et al., 1999; Gustin et al., 2019; Huang et al., 2012; Maruszczak et al., 2017; Miller et al., 2019). This material is purchased in sheets (Pall Corporation) that were cut into 47 mm diameter discs using a steel cutting die (see Huang et al., 2013 and SI for additional information). Miller et al. (2019) showed GEM uptake by the CEM material was negligible. CEM were digested in 50 mL centrifuge tubes (Falcon®, Corning Inc.) in which they were collected and stored, and Hg was quantified using a Tekran® 2600. Analyses for the UNR-RMAS employed the peristaltic pump model, whereas the UNR-RMAS 2.0 used the in-vial sparge model; specifications of the in-vial sparge method are detailed in the SI.

The second membrane type is a nylon polyamide membrane (0.2 µm pore size, 47 mm diameter; Sartorius Stedium). This membrane is used for thermal desorption analyses with the objective to identify the collected RM compounds. The nylon material maintains structure during the thermal desorption cycle, unlike the CEM material that degrades significantly and passivates the Tekran® 2537 gold cartridges. The results of Huang et al. (2013) demonstrated that when used alongside one another, the CEM can be used to quantify RM and the nylon membrane can be used to identify the RM compounds collected.

For both membrane types, the upstream (A) membrane collected most of the RM and the downstream (B) membrane was used to collect any RM that breaks through the A membrane. Percent breakthrough was calculated as follows:

$$\% \text{ breakthrough} = \frac{(B - \text{blank})}{((B - \text{blank}) + (A - \text{blank}))} \times 100 \quad \text{Equation 1}$$

Thermal desorption of the downstream nylon membranes from the UNR-RMAS had very low concentrations and did not provide meaningful data for identification of RM compounds. Thus, the UNR-RMAS 2.0 method was used to quantify the total Hg concentration on the downstream nylon membranes using the Tekran® 2600 (average: 0.092 pg Hg; n = 126). In addition, comparison of thermal desorption of nylon membranes and analyses of nylon membranes by Tekran® 2600 yielded similar Hg concentrations (discussion in SI).

2.3. Improvements to the UNR-RMAS

Significant changes were made to the UNR-RMAS. With the original design, upstream and downstream membranes were 15 cm apart and connected by 6.35 mm Teflon® outer diameter tubing, and filter holders were not protected from direct sunlight. The flow rate was difficult to manage. Samples membranes were deployed for 2 weeks and stored in glass jars. The UNR-RMAS 2.0 uses multiple-stage filter packs, a protective metal shield, a two-pump design, and critical flow orifices (CFO; Teledyne) to restrict flow to a constant rate of 1 Lpm. The deployment time has been reduced from 2- to 1- week, and storage vessels were changed to centrifuge tubes. Manufacturer information and part numbers for components of the UNR-RMAS 2.0 are provided in the supporting information (Table SI 1).

Filter holders were upgraded to multi-stage perfluoroalkoxy alkane (PFA) filter holders that hold one, two or three membranes 5 mm apart

(Saville). Contamination risk is reduced using the multi-stage filter holder due to less surface area for GOM and PBM to potentially sorb to surfaces.

Filter holders are housed underneath a custom designed anodized aluminum weather shield (Deluxe Welding, Reno, Nevada) mounted 1 m above the ground. The custom designed shield was constructed using an aluminum plate 56 cm wide x 35.5 cm bent at 45° and 90° angles resulting in 15, 13, and 7.5 cm segments (Fig. SI 2). Six holes are drilled through the top of the shield at 7.6 cm intervals to hold the CFO assemblies securely. Filter holders are connected to the shield by 5 cm long Teflon® 6.35 mm outer diameter tubes that connect to the CFO

assemblies.

Flow rate management has been simplified with CFO that control flow at 1 Lpm, and 2 diaphragm vacuum pumps (KNF Neuberger Inc., 34 Lpm capacity; we recommend finding an alternate pump). CFO are housed in a steel tube with a particle filter frit at the inlet to prevent clogging (Fig. 1a). Bev-a-line® tubing is used to connect the CFO for three sample lines to a 4-way union with the fourth port connected to one vacuum pump. Ports 1–3 are sampled by one pump, and ports 4–6 by another. The two-pump system with CFO provided more consistent flow than one pump for each line. The positioning of the filter membrane types was alternated so that: 1) two samples of one membrane type and 1

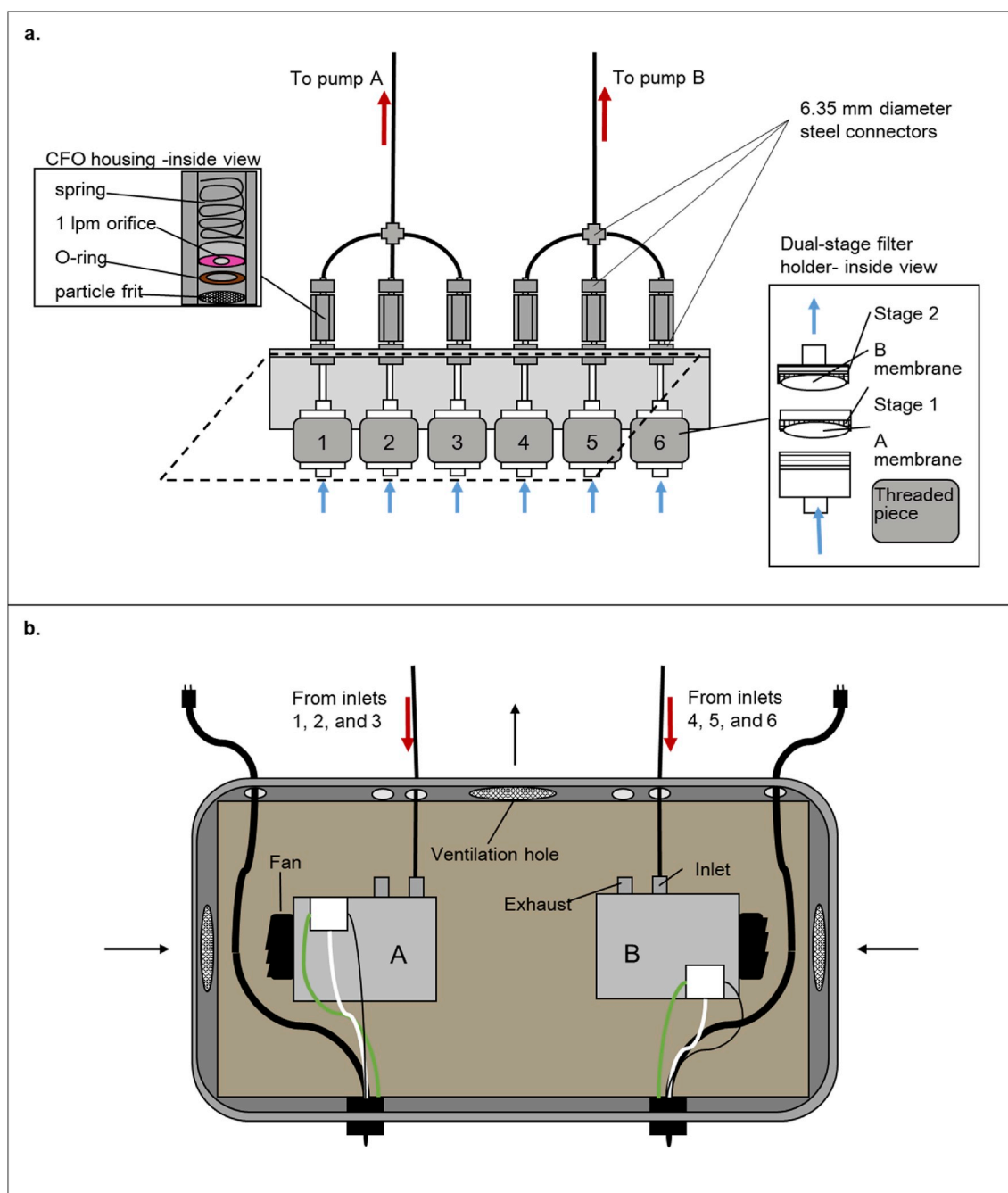


Fig. 1. a) Dotted black parallelogram represents the front of the aluminum shield. Blue arrows represent nominal air flow rate of 1 Lpm. Red arrows represent the sum of the three-sample inlet air flow rates pulled by each pump, in this case 3 Lpm. The dual-stage filter holders, numbered 1–6, are sealed by tightening the threaded plastic grey piece. b) Top down view of pump box. Black arrows represent ventilation flow through the box. Colored wires represent power to the power switch, ground wires etc. Ventilation ports are covered with fine mesh to prevent debris from entering the box. (For interpretation of the references to colour in this figure legend, the reader is referred to the Web version of this article.)

sample of the other membrane type would continue to be sampled in case of a pump failure, reducing the risk of losing all of one membrane type in such an event; and 2) to minimize the bias of air flow coming into the manifold from the middle and sides. Filter holders 1, 3, and 5 house CEM, and filter holders 2, 4, and 6 house nylon membranes (Fig. 1a).

A pump box (Husky® plastic toolbox) provides weather-resistant protection for the pumps and functions as an easy-to-transfer unit. The pump box is equipped with mounting brackets custom fit to securely attach the pumps to the particle board bottom (Fig. 1b). The pumps are wired to toggle switches mounted on the side of the box to allow for simple turning on and off the pumps. The pump box has air ventilation holes covered with particle filters to reduce debris from entering the box, and holes for the samples lines and power cables to lead out while the pump box is closed. For this study, the pump box was housed in a trailer with the sample lines leading outside to the manifold.

Flow rates for each line were measured at the sample air inlet of each of the 6 sample ports (Fig. 1a) at the beginning and end of the deployment period using a TetraCal® flow calibrator. Flow rates ranged from 0.6 to 0.9 Lpm during the campaign and deviated less than 0.1 Lpm from the beginning to the end of individual deployments. The mean of these flow rates was used to calculate the volume of air that was pulled through each membrane. All flow rates were recorded as standard flow. Deployments were 2 weeks long beginning in March 2018. The deployment time was then reduced to 1 week in September 2018 until the end of the experiment in March 2019. Sample membranes were analyzed within 1 month of collection.

2.4. Modifications to the thermal desorption method

Different Hg compounds are desorbed from the nylon membrane at different temperatures, due to differing chemical structures and bond strengths. This is similar to work done using soils and coal combustion materials (Lopez-Anton et al., 2010; Rumayor et al., 2013, 2015; Yang et al., 2017). Hg(II) compounds were identified by comparing the peak release temperatures with standard curves developed for each compound (Gustin et al., 2015, 2016; Huang et al., 2013). Nylon membranes were heated in a tube furnace to release RM. Hg released then travelled through a pyrolyzer that reduced the RM to GEM, and then was measured by the Tekran® 2537A (Fig. SI 3). In the initial design, the pyrolyzer temperature and temperature ramp of the furnace was not optimized. The tube furnace program was 65 min long and the rate of temperature change over time was not consistent during the entire cycle. The temperature reported by the tube furnace was lower than the actual temperature inside the membrane desorption environment, and therefore the true peak desorption temperature for a given compound was misrepresented.

The thermal desorption system of UNR-RMAS 2.0 used an improved pyrolyzer (Miller et al., 2019) that maintained stable temperature set to 387.7 °C. Testing the pyrolyzer temperature at 387.7, 450, 650, and 900 °C showed no significant difference in profile shape or total amount of Hg measured by the downstream Tekran® 2537A (details in SI; Fig. SI 4). The UNR-RMAS 2.0 thermal desorption method was simplified to have a consistent rate of change with 5 min holding temperatures at the beginning and end of the program. The tube furnace was programmed to start at 50 °C for 5 min, then increased to 200 °C over the course of 75 min (5 °C change for every 2.5 min cycle of the Tekran® 2537A), then held at 200 °C for 5 min. For additional details see the SI.

The tube furnace was calibrated every 6 weeks. The calibration was very stable and did not change. Calibration of tube furnace temperatures using a thermocouple showed that the actual temperature on the wall of the tube furnace that is where the membrane rests during analysis was significantly lower than the display of the tube furnace between 4 °C (minimum difference) and 17 °C (maximum difference) (Fig. SI 5). This was true for both the temperature ramp program used to generate the standard curves in Huang et al. (2013) and for the UNR-RMAS 2.0 improved temperature ramp. All samples analyzed using UNR-RMAS 2.0

methods were calibrated to reflect the actual temperature inside the tube furnace.

2.5. Thermal desorption method comparison

To demonstrate the effect of changing the thermal desorption temperature ramp between the UNR-RMAS and UNR-RMAS 2.0, replicate field samples were thermally desorbed using both tube furnace programs (Fig. SI 6). Six nylon membranes were deployed in the UNR-RMAS 2.0, collecting ambient air, over a 1-week period. Three of the samples were analyzed using the UNR-RMAS tube furnace program and plotted using the furnace display temperature, following the procedure from Huang et al. (2013), and three samples were analyzed using the improved UNR-RMAS 2.0 program and plotted using the actual temperature inside the tube furnace measured by thermocouple. This experiment was repeated three times (three 1-week deployments). The area under each thermal desorption curve was calculated using the “auc” function in the MESS package (Ekstrom, 2019) in R Statistical Package.

2.6. Thermal desorption peak deconvolution

A quantification method was developed to resolve the individual GOM compound peaks from the thermal desorption profiles. Reference GOM profiles were generated from solid phase mercury compounds (HgBr₂, HgCl₂, HgN₂O₆•H₂O, HgSO₄, and HgO) and elemental Hg, as well as methylmercury chloride directly added to membranes (Alfa Aesar; CH₃HgCl 1000 ppm in water). Based on previous studies (Gustin et al., 2015, 2016; Huang et al., 2013), and calibration of temperature to reflect the actual temperature of desorption from the nylon membrane, GOM compounds were defined by peaks in the following ranges: 80–85 °C for [-O], 90–110 °C for [-Br/Cl], 125–135 °C for [-N], 150–155 °C for [-S], and 180–190 °C for methylmercury (MeHg) or organic bound compounds. The profile shape for MeHg developed in Gustin et al. (2016) was made with a liquid standard, and for interpreting thermal desorption results they are described as organic compounds.

To quantify the RM compounds measured using thermal desorption, compound peaks were considered to be Gaussian. The curve fitting function in MATLAB R2018a was used to deconvolute the thermal desorption profiles into individual compound peaks with peak temperatures fixed within a defined range. The model result is the integral of the area of each peak (unit: °C × ng × m⁻³). An alternative approach is to convert the thermal desorption temperature to time, resulting in the conversion of the Hg concentration data (ng m⁻³) to Hg release rate (pg min⁻¹) based on the thermal desorption Tekran 2537 sampling rate (1 Lpm), and calculating the integral of peak area (unit: pg). The second integration method was most useful, as the concentration of each RM compound, in pg m⁻³, can be directly calculated by dividing the peak area integral by the sampling volume of the UNR-RMAS 2.0 for the sampling duration. The second method was used here.

2.7. Ion chromatography

Ion chromatography (IC) was used to quantify the major anions associated with nylon membranes. This allowed for determining if RM compounds thought to be on the membranes based on thermal desorption peak interpretations were similar to anions measured in the membrane extract and provided information on chemistry of air masses at the site. This method helped elucidate the possible Hg compounds present on nylon membranes by quantifying the dominant ions present. This was not a direct quantification method, as ions present may not have been exclusively associated with Hg.

One of three replicate nylon membranes from select UNR-RMAS 2.0 deployments were extracted in 20 mL of 18.2 MΩ water, shaken, and set to rest for 4 h or more. Digestate was filtered through a 0.45 μm nylon filter to remove membrane particles. The filtrate was analyzed using a

Dionex™ 3000 ion chromatography system equipped with a Dionex™ AS-19 column. Programmed analyses were a total of 33 min long for each sample. The potassium hydroxide eluent concentration was 15.0 mM for 18 min, then increased to 40.0 mM for an additional 12 min, then the concentration was lowered back to 15.0 mM for 3 min. Blank membranes were analyzed as controls to quantify the contribution of the membrane material to the anion concentrations. Concentrations measured in the blank membranes digestate was subtracted from the concentrations in sample membrane digestate. Membranes permeated with compounds from HgBr₂, HgCl₂, and HgN₂O₆·H₂O permeation tubes were used to verify the method and ensure the anions known to be associated with the Hg compound were detectable. Measured anions

included fluoride, chloride, bromide, sulfate, nitrate, nitrite, and phosphate. Concentrations of these ions were verified by seven anion standard curves (Dionex™ 057590) daily at the start and end of each analysis. The standard curves were used to calibrate the peak areas reported by the instrument, then concentrations were calculated in ppb.

Results of IC analyses were compared with those of the peak deconvolution to see if anions associated with Hg were consistent with those compounds isolated by peak deconvolution.

2.8. Tekran® speciation system

The Tekran® 2537/1130 system measured GEM and GOM,

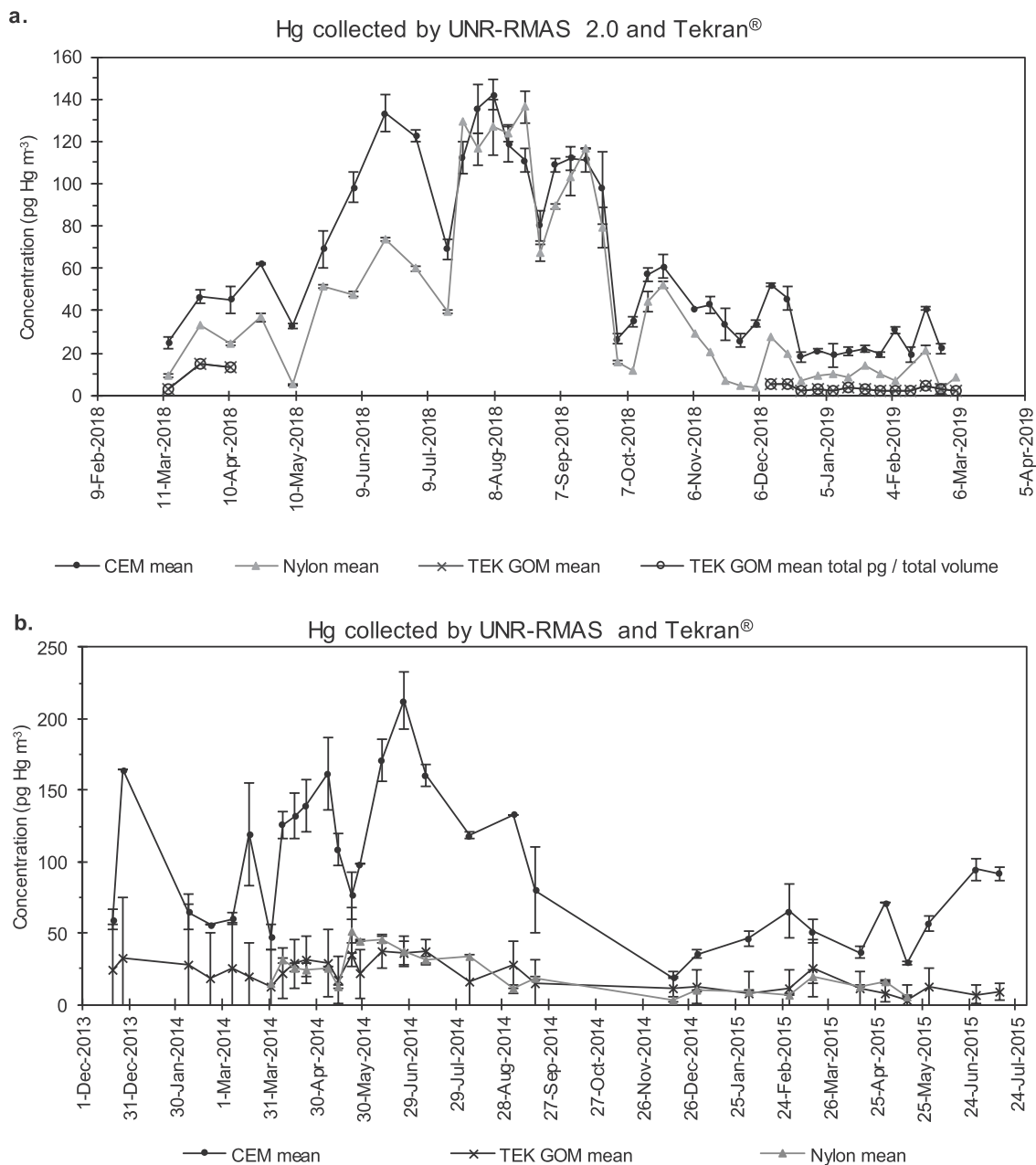


Fig. 2. Mean concentrations of Hg measured on the CEM, nylon membranes, and Tekran® GOM measured during (a) UNR-RMAS 2.0 deployments this study and (b) UNR-RMAS data collection during 2014–2015. All concentration units are pg Hg m⁻³. Error bars represent standard deviation. Error bars are shown for samples where n ≥ 3. CEM and nylon membrane samples were deployed for two weeks for all deployments and then decreased to one week beginning in September 2018. In panel a., the open circles represent GOM concentrations on the denuder calculated with outside flow measurements. These overlap with the reported concentrations by the instrument (black X).

respectively. The fact that no 1135 unit was used may have resulted in underestimation of RM. The sampling inlets for UNR-RMAS 2.0 and Tekran® were at the same height, 1 m from the ground, and 2 m apart (Fig. SI 1). For a description of the Tekran® sampling system please see the SI. In addition, Tekran® does not take into account the low bias that occurs due to data processing by the Tekran® software as indicated by Ambrose (2017). A low bias occurs at concentrations of 1–2 ng m⁻³. This also impacts GOM and PBM measurements that are often <5 pg. However, given issues with the 1130 and 1135 units, correcting these data would not matter.

During the two sampling campaigns, Tekran® systems were operated the same. Air first passed through an elutriator designed to remove particles >2.5 µm, then through a KCl-coated denuder in the 1130 unit followed by a short line into a glass fiber filter, then through a heated line (50 °C; 7.6 m) at 5.5 Lpm. The lower flow rate does not affect denuder performance, but increased the aerodynamic diameter cut point of the impactor to 3.0 µm (Chow, 1998; Lyman et al., 2007).

To ensure that the mean GOM concentration measured with the Tekran® 1130 system over the one-week sampling intervals was representative of actual GOM collected by the denuder, the total mass of Hg in pg collected by the denuder was divided by the total volume of air that passed through the Tekran® system during GOM collection as calculated using flow measurements at the inlet (Fig. 2 a). These values were not significantly different from the mean concentrations of GOM reported by the Tekran® (ANOVA, $p = 0.995$). Thus, mean GOM concentration in pg m⁻³ determined by averaging the concentrations over time was compared with the UNR-RMAS 2.0 data. This is consistent with other studies that report mean Tekran® results in comparison with alternate Hg measurement systems (Ambrose et al., 2013; Gustin et al., 2013; Lyman et al., 2016; Maruszczak et al., 2017; Zhang et al., 2016). Sample t-tests were performed in Excel and ANOVA tests were performed in R Statistical Package v.3.4.1.

3. Results and discussion

3.1. Concentrations measured by CEM, nylon membranes, and Tekran® system

UNR-RMAS 2.0 CEM and nylon membranes collected more RM (29 ± 12 pg m⁻³; 14 ± 9 pg m⁻³) than the Tekran® 1130 collected GOM (5 ± 4 pg m⁻³) during the limited time they overlapped during the 2018–2019 experiment (Fig. 2 a.; the gap in Tekran® data from April to December was due to instrument failure). Concentrations measured by the CEM were 3.3–9.7 times higher than those measured by the Tekran®. This is within the range 1.7–13 times reported by Gustin et al. (2016). Comparing the trends between seasons of sampling (Fig. 2 a and b) showed that mean GOM measured by the Tekran® was higher in Reno during summer 2014 (24 ± 15 pg Hg m⁻³) relative to winter 2014–2015 (14 ± 15 pg Hg m⁻³). This same trend was observed using the Tekran® system in past studies at this field site. Mean summer GOM was 51 pg m⁻³ and 7 pg m⁻³ during winter 2004–2007 (Peterson et al., 2009). Summer GOM concentrations were 36 pg m⁻³ and 4 pg m⁻³ in winter on average from 2007 to 2009 (Lyman et al., 2007 (Fig. 2)).

In 2018–2019, RM concentrations on the CEM increased from 54 ± 4 pg m⁻³ in the spring to 112 ± 7 pg m⁻³ in the summer. Concentrations decreased in the fall to 41 ± 4 pg m⁻³ and RM concentrations were lowest in winter at 23 ± 2 pg m⁻³. The CEM captured more RM on average during the year 2018–2019 than did the nylon (nylon recovery was 69% of that recovered by CEM), but during the summer, nylon membrane Hg concentrations (97 ± 5 pg m⁻³) increased to 87% recovery relative to the CEM. Three summer deployments had higher nylon membrane Hg concentrations than CEM concentrations (Fig. 2 a). This trend indicates that the nylon membranes were more efficient at collecting summertime RM compounds that were primarily halogen based. Field data collected over a year at NOAA Mauna Loa Observatory, Hawaii; Valley Road Greenhouse, Reno, Nevada; Piney Reservoir,

Maryland; and Horsepool, Utah demonstrated that nitrogen compounds are not as efficiently collected by nylon membranes as the other compounds (Luippold et al. in progress).

Percent recovery of nylon compared to CEM during the 2014–2015 study was 24% for the year on average and 23% during summer. The discrepancy between 2014–2015 and 2018–2019 CEM versus nylon membrane comparisons could be due to 1) some change in manufacture of the nylon membranes or 2) differences in atmospheric chemistry. Potential RM compounds collected on the nylon membranes are discussed in the next section.

Coefficients of variation for replicate membranes ($n = 3$ for each sampling period) of total Hg collected by CEM and nylon membranes of the UNR-RMAS 2.0 system, $8.2\% \pm 4.7\%$ ($n = 126$) and $6.3\% \pm 5.0\%$ ($n = 103$), respectively, were less than the coefficients of variation for CEM, $12.3\% \pm 12.8\%$ ($n = 149$), and nylon, $12.8\% \pm 12.4\%$ ($n = 105$) of the UNR-RMAS. This demonstrates that the UNR-RMAS 2.0 methods improved sample replication.

Breakthrough of Hg through the upstream membrane to the downstream membrane was on average lower for UNR-RMAS 2.0 samples than UNR-RMAS. The average breakthrough for CEM of the UNR-RMAS 2.0 samples was 13.1% and for nylon membranes was 7.4%. The breakthrough for UNR-RMAS samples was 25.5% for CEM and 13.9% for nylon. The better performance associated with the UNR-RMAS 2.0 is due to using the multistage filter packs.

3.2. Thermal desorption profiles

Comparing the UNR-RMAS and UNR-RMAS 2.0 thermal desorption tube furnace programs by analyzing replicate samples under the two treatments showed that the sample peaks desorbed at different temperatures for each method, with the UNR-RMAS 2.0 method peaking ~15 °C lower than the UNR-RMAS. When the actual temperature of the tube furnace is used to plot the samples desorbed using the UNR-RMAS temperature ramp program, there was no significant difference between the two methods (ANOVA $p = 0.916, 0.693, 0.914$; Fig. SI 6 d-f).

Thermal desorption profiles from 2014 to 2015 (Gustin et al., 2016) UNR-RMAS deployment nylon membranes are shown in Fig. 3 column 1 (a-e) with pg Hg released plotted against original tube furnace display temperatures (black line) and the calibrated temperatures (orange line). The difference between these curves in each plot shows shifted peaks by approximately 15 °C to the left when the actual temperature of the tube furnace was used to graph the results. Desorption profiles from the UNR-RMAS 2.0 (Fig. 3, column 2) showed more consistent replication of sample membranes, as indicated by the blue curves in column 2 compared to the grey curves in column 2. Coefficient of variation of the Hg released from the nylon membranes shown in Fig. 3 was $9.7\% \pm 1.2\%$ ($n = 15$) on average, for thermal desorption profiles ($n = 3$ for each sample) for the UNR-RMAS 2.0 samples and $21.4\% \pm 9.2\%$ ($n = 15$) for the UNR-RMAS samples. This indicates that the overall replication between samples was better for nylon membrane samples collected and analyzed using UNR-RMAS 2.0 methods compared to the UNR-RMAS method.

Additionally, the peak area under the thermal desorption curves did not change significantly between methods. The area under the curve for desorption profiles in Fig. SI 6 was not significantly different in weeks 1 and 3 (95% confidence; two-sample, two tail t-tests assuming equal variances, $p = 0.850, 0.019, 0.804$ for replication weeks 1, 2, and 3, respectively). Because the temperature of peak release and the total Hg released by membranes using each method were similar, nylon membranes analyzed in 2014–2015 can be directly compared with the 2018–2019 UNR-RMAS 2.0 results.

Desorption peaks based on actual temperatures of the tube furnace are approximately 83 °C for oxide (O) compounds, 90–110 °C for bromide (Br) and chloride (Cl) compounds, 130 °C for nitrogen (N) compounds, 150 °C for sulfur (S) compounds, and 180–190 °C for what has been considered organic compounds. The investigation of thermal

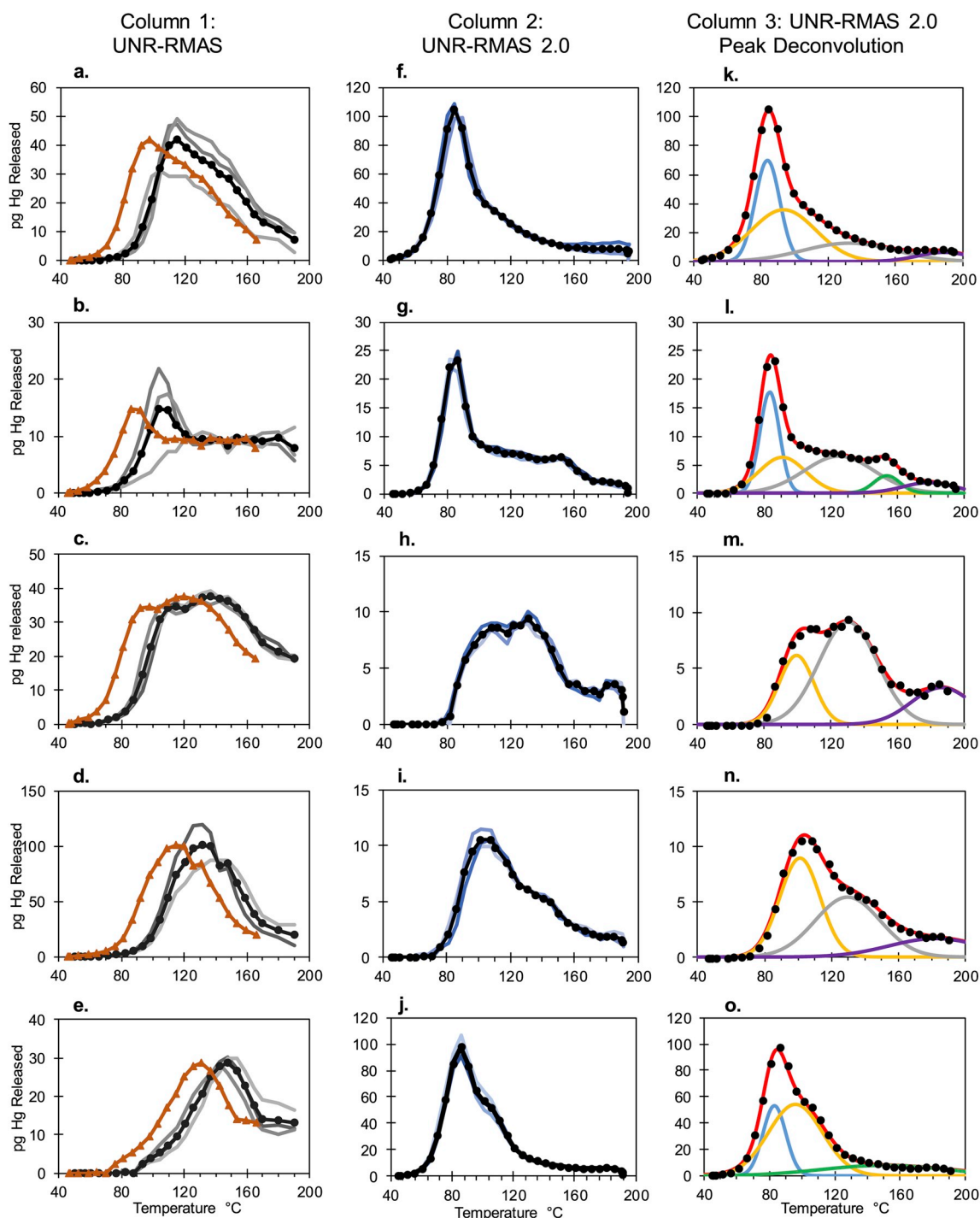


Fig. 3. Column 1 (a–e) shows UNR-RMAS thermal desorption profiles from 2014 to 2015. The grey lines are replicate profiles of sample membranes ($n = 3$) and the black line with dots represents the average profile for the deployment. The orange line with triangles is the average profile plotted to reflect the actual temperature of the tube furnace. In Column 2 (f–j) are UNR-RMAS 2.0 samples from 2018 to 2019 plotted using actual temperature of the tube furnace. The blue lines represent replicate samples and the black line with dots represent the average profile of the replicates ($n = 3$). Samples in columns 1 and 2 were chosen because of their similar shapes. For example: samples b and g are similar profiles in shape and peak desorption temperature when compared with calibrated temperatures. Column 3 (k–o) shows the results of integrating peaks of the profiles in column 2. Legend: black = average profile points; red = fitted curve; blue = O; yellow = Br/Cl; grey = N; green = S; purple = MeHg. (For interpretation of the references to colour in this figure legend, the reader is referred to the Web version of this article.)

desorption trends for 2018–2019 demonstrated that S and organic-based Hg compounds were most prevalent in winter (Table SI 2). These S and organic compounds were accompanied by O-based compounds in the winter. In spring, the most common compounds were Br/Cl compounds. O-based compounds were present late summer into winter. S-based compounds followed a similar pattern to the O compounds, where they

were present generally in all seasons excluding late spring and summer. Thermal desorption profiles from 2014 to 2015 UNR-RMAS samples showed Br/Cl based compounds in the winter and spring, with no instances of these compounds in summer or fall. S and organic compounds were seen sporadically throughout the year. N compounds were shown throughout the year, but were not present in late fall. O-based

compounds rarely appeared in 2014–2015 samples. During the summer of 2018, when total Hg on the nylon membranes was similar or greater than on the CEM, the dominating compounds were O and Br/Cl based. N and S compounds appeared in addition to these compounds in late summer.

3.3. Peak deconvolution and ion chromatography

Deconvolution of the UNR-RMAS 2.0 thermal desorption peaks in Fig. 3, column 2 resulted in the curves shown in column 3. These desorption profiles were each characterized by a major peak. For profiles (k), (l), and (o), these major peaks desorb in the range for O-based compounds. Profiles (m) and (n) major peaks were Br/Cl with additional N peaks. Based on peak deconvolution quantifications (Table 1), dominant Hg compounds in these samples by proportion of total pg Hg were Br/Cl, N, Br/Cl for samples (k), (l), (o), respectively. Profiles (m) and (n) were proportionally N dominated (56.5%; 40.7%).

Nylon membranes from select time periods were analyzed with one replicate by IC and 2 replicates by thermal desorption. In each of the samples analyzed with IC, sulfate made up a large proportion of total anions detected (20–93%), as did nitrate (0–45%) and chloride (0–51%). Fluoride, nitrite, phosphate, and bromide had low concentrations (0–11% of total anions).

Three cases where both IC results and peak deconvolution results were available were compared. Deconvolution of the peaks for replicates thermally desorbed and corresponding anion concentrations are shown in Fig. SI 7. Sample (a) was dominated by N compounds, representing 61% of the total sample peak area. The IC results of (a) showed the ions found on the membrane were 30.7% nitrate and 49.2% sulfate of total ions detected. Sample (b) was predominantly comprised of organic Hg or MeHg-type compounds according to the peak deconvolution (37.0%), and sulfate was the main ion measured by IC, with 45.6% of ions quantified. Sample (c) was 69.7% S-associated based on the peak deconvolution and was dominated by sulfate ions (52.2% of total ions measured). Peak deconvolutions and IC analysis results generally agreed. These methods may be viable techniques for identifying and quantifying specific RM compounds collected on nylon membranes.

4. Conclusions

The UNR-RMAS 2.0 collected more RM than the Tekran® system, had improved sample replication compared to a previous system, and increased the temporal resolution for RM sampling from 2 to 1-week. The thermal desorption method was refined by calibrating samples to actual tube furnace temperatures, simplifying the tube furnace temperature program, and increasing the measurement resolution of released Hg. The peak deconvolution method paired with ion chromatography is a significant step towards better understanding RM compounds on nylon membranes. Gustin et al. (2019) demonstrated that the UNR-RMAS 2.0 is a viable system available for RM, GOM, and PBM quantification and compound identification.

There are some limitations and uncertainties that need to be considered with respect to the UNR-RMAS 2.0 method that need further investigation. Potential reactions on the membrane, with organic and sulfate aerosols and particles collected on the membrane. Emission of GEM from the membranes through reduction of RM could reduce the concentration of RM on the membranes resulting in under estimation of compounds. There are a limited number of compounds for which we can develop calibration profiles and these may not reflect compounds in the atmosphere. Development of a GC-MS system that would allow for identification would be very useful for understanding the exact compounds present. We are currently investigating if reactions on the membranes in ambient air could generate compounds observed. Our work using multiple lines of evidence (i.e., ion chromatography, back trajectory analyses, criteria air pollutant data and meteorology) suggest that the compounds present are derived from the air not due to reactions

Table 1

Results of UNR-RMAS 2.0 thermal desorption peak deconvolution showing the peak temperature, the GOM compounds present based on calibrated profiles, the peak area, and the relative percent of each compound in the sample. Samples 1–5 correspond to the profiles in column 3 of Fig. 3(k–o). The total pg Hg for each peak is shown with the proportion of the GOM compound relative to the total peak area.

| Sample No. | Peak No. | Peak Temp | GOM Form | Peak Area | Proportion |
|--------------|----------|-----------|----------|-----------|------------|
| | | | | pg Hg | % |
| Sample 1 (k) | P1 | 84 | O | 257 | 31.2 |
| | P2 | 93 | Br/Cl | 345 | 42.0 |
| | P3 | 132 | N | 173 | 21.1 |
| | P4 | 189 | MeHg | 47 | 5.8 |
| Sample 2 (l) | P1 | 83 | O | 52 | 27.4 |
| | P2 | 91 | Br/Cl | 44 | 22.9 |
| | P3 | 125 | N | 69 | 35.9 |
| | P4 | 154 | S | 12 | 6.4 |
| | P5 | 179 | MeHg | 14 | 7.3 |
| Sample 3 (m) | P1 | 100 | Br/Cl | 32 | 22.5 |
| | P2 | 130 | N | 80 | 56.5 |
| | P3 | 186 | MeHg | 30 | 21.0 |
| Sample 4 (n) | P1 | 101 | Br/Cl | 54 | 41.1 |
| | P2 | 130 | N | 53 | 40.7 |
| | P3 | 182 | MeHg | 24 | 18.2 |
| Sample 5 (o) | P1 | 83 | O | 186 | 23.9 |
| | P2 | 96 | Br/Cl | 448 | 57.6 |
| | P3 | 150 | S | 144 | 18.5 |

occurring on membrane surfaces (Luippold et al., in progress).

Authors contributions

Addie Luippold a Master's Degree candidate was responsible for collecting the data and compiling the paper.

Mae Gustin supervised the graduate student while doing the work and guided the writing and data analyses.

Sarah Dunham-Cheatham helped the graduate student with the experiments and data compilation, as well as helped with writing and editing the paper.

Lei Zhang developed the deconvolution method for the thermal desorption profiles and did this data analyses. He also helped with writing and editing the paper.

Declaration of competing interest

The authors declare that they have no known competing financial interests or personal relationships that could have appeared to influence the work reported in this paper.

Acknowledgements

This work was funded by NSF Grant 629679 from the National Science Foundation Atmospheric Chemistry Program. Ion chromatography analyses were made possible through help from Dr. Glenn Miller and Riley Dunavent. We also thank the Gustin lab undergraduates Margarita Vargas Estrada, Molly Willoughby, and Samir Gulati. We thank the anonymous reviewers for their feedback that helped to improve this manuscript.

Appendix A. Supplementary data

Supplementary data to this article can be found online at <https://doi.org/10.1016/j.atmosenv.2020.117307>.

References

- Ambrose, J.L., 2017. Improved methods for signal processing in measurements of mercury by Tekran (R) 2537A and 2537B instruments. *Atmos. Meas. Tech.* 10, 5063–5073.
- Ambrose, J.L., Lyman, S.N., Huang, J.Y., Gustin, M.S., Jaffe, D.A., 2013. Fast time resolution oxidized mercury measurements during the Reno atmospheric mercury intercomparison experiment (RAMIX). *Environ. Sci. Technol.* 47, 7285–7294.
- Ariya, P.A., Amyot, M., Dastoor, A., Deeds, D., Feinberg, A., Kos, G., et al., 2015. Mercury physicochemical and biogeochemical transformation in the atmosphere and at atmospheric interfaces: a review and future directions. *Chem. Rev.* 115, 3760–3802.
- Caldwell, C.A., Swartzendruber, P., Prestbo, E., 2006. Concentration and dry deposition of mercury species in arid south central New Mexico (2001–2002). *Environ. Sci. Technol.* 40, 7535–7540.
- Castro, M.S., Moore, C., Sherwell, J., Brooks, S.B., 2012. Dry deposition of gaseous oxidized mercury in Western Maryland. *Sci. Total Environ.* 417, 232–240.
- Chow, JaWJ., 1998. Guideline on Speciated Particulate Monitoring.
- Ebinghaus, R., Jennings, S.G., Schroeder, W.H., Berg, T., Donaghy, T., Guentzel, J., et al., 1999. International field intercomparison measurements of atmospheric mercury species at Mace Head, Ireland. *Atmos. Environ.* 33, 3063–3073.
- Ekstrom, C.T., 2019. MESS: miscellaneous esoteric statistical scripts. R package version 0.5.5. <https://github.com/ekstroem/MESS/issues>.
- Environmental Protection Agency (EPA), 2002. Method 1631, Revision E: Mercury in Water by Oxidation, Purge and Trap, and Cold Vapor Atomic Fluorescence Spectrometry, p. 45. United States.
- Gustin, M.S., Huang, J.Y., Miller, M.B., Peterson, C., Jaffe, D.A., Ambrose, J., et al., 2013. Do we understand what the mercury speciation instruments are actually measuring? Results of RAMIX. *Environ. Sci. Technol.* 47, 7295–7306.
- Gustin, M.S., Amos, H.M., Huang, J., Miller, M.B., Heidecorn, K., 2015. Measuring and modeling mercury in the atmosphere: a critical review. *Atmos. Chem. Phys.* 15, 5697–5713.
- Gustin, M.S., Pierce, A.M., Huang, J.Y., Miller, M.B., Holmes, H.A., Loria-Salazar, S.M., 2016. Evidence for different reactive Hg sources and chemical compounds at adjacent valley and high elevation locations. *Environ. Sci. Technol.* 50, 12225–12231.
- Gustin, M.S., Dunham-Cheatham, S.M., Zhang, L., 2019. Comparison of 4 methods for measurement of reactive, gaseous oxidized, and particulate bound mercury. *Environ. Sci. Technol.* 53 (24), 14489–14495. <https://doi.org/10.1021/acs.est.9b04648>.
- Huang, J.Y., Gustin, M.S., 2015a. Uncertainties of gaseous oxidized mercury measurements using KCl-coated denuders, cation-exchange membranes, and nylon membranes: humidity influences. *Environ. Sci. Technol.* 49, 6102–6108.
- Huang, J.Y., Gustin, M.S., 2015b. Use of passive sampling methods and models to understand sources of mercury deposition to high elevation sites in the western United States. *Environ. Sci. Technol.* 49, 432–441.
- Huang, J.Y., Choi, H.D., Landis, M.S., Holsen, T.M., 2012. An application of passive samplers to understand atmospheric mercury concentration and dry deposition spatial distributions. *J. Environ. Monit.* 14, 2976–2982.
- Huang, J.Y., Miller, M.B., Weiss-Penzias, P., Gustin, M.S., 2013. Comparison of gaseous oxidized Hg measured by KCl-coated denuders, and nylon and cation exchange membranes. *Environ. Sci. Technol.* 47, 7307–7316.
- Huang, J.Y., Miller, M.B., Edgerton, E., Gustin, M.S., 2017. Deciphering potential chemical compounds of gaseous oxidized mercury in Florida, USA. *Atmos. Chem. Phys.* 17, 1689–1698.
- Lopez-Anton, M.A., Yuan, Y., Perry, R., Maroto-Valer, M.M., 2010. Analysis of mercury species present during coal combustion by thermal desorption. *Fuel* 89, 629–634.
- Lyman, S.N., Gustin, M.S., Prestbo, E.M., Marsik, F.J., 2007. Estimation of dry deposition of atmospheric mercury in Nevada by direct and indirect methods. *Environ. Sci. Technol.* 41, 1970–1976.
- Lyman, S.N., Jaffe, D.A., Gustin, M.S., 2010. Release of mercury halides from KCl denuders in the presence of ozone. *Atmos. Chem. Phys.* 10, 8197–8204.
- Lyman, S., Jones, C., O'Neil, T., Allen, T., Miller, M., Gustin, M.S., et al., 2016. Automated calibration of atmospheric oxidized mercury measurements. *Environ. Sci. Technol.* 50, 12921–12927.
- Maruszczak, N., Sonke, J.E., Fu, X.W., Jiskra, M., 2017. Tropospheric GOM at the pic du Midi observatory—correcting bias in denuder based observations. *Environ. Sci. Technol.* 51, 863–869.
- MATLAB and Statistics Toolbox. Mathworks, Inc., Natick, Massachusetts, United States.
- McClure, C.D., Jaffe, D.A., Edgerton, E.S., 2014. Evaluation of the KCl denuder method for gaseous oxidized mercury using HgBr₂ at an in-service AMNet site. *Environ. Sci. Technol.* 48, 11437–11444.
- Miller, M.B., Dunham-Cheatham, S.M., Gustin, M.S., Edwards, G.C., 2019. Evaluation of cation exchange membrane performance under exposure to high Hg-0 and HgBr₂ concentrations. *Atmos. Meas. Tech.* 12, 1207–1217.
- Peterson, C., Gustin, M., Lyman, S., 2009. Atmospheric mercury concentrations and speciation measured from 2004 to 2007 in Reno, Nevada, USA. *Atmos. Environ.* 43, 4646–4654.
- Pierce, A.M., Gustin, M.S., 2017. Development of a particulate mass measurement system for quantification of ambient reactive mercury. *Environ. Sci. Technol.* 51, 436–445.
- Rumayor, M., Diaz-Somoano, M., Lopez-Anton, M.A., Martinez-Tarazona, M.R., 2013. Mercury compounds characterization by thermal desorption. *Talanta* 114, 318–322.
- Rumayor, M., Lopez-Anton, M.A., Diaz-Somoano, M., Martinez-Tarazona, M.R., 2015. A new approach to mercury speciation in solids using a thermal desorption technique. *Fuel* 160, 525–530.
- Talbot, R., Mao, H.T., Feddersen, D., Smith, M., Kim, S.Y., Sive, B., et al., 2011. Comparison of particulate mercury measured with manual and automated methods. *Atmosphere* 2, 1–20.
- Yang, J.P., Ma, S.M., Zhao, Y.C., Zhang, J.Y., Liu, Z.H., Zhang, S.H., et al., 2017. Mercury emission and speciation in fly ash from a 35 MWth large pilot boiler of oxyfuel combustion with different flue gas recycle. *Fuel* 195, 174–181.
- Zhang, L.M., Wu, Z.Y., Cheng, I., Wright, L.P., Olson, M.L., Gay, D.A., et al., 2016. The estimated six-year mercury dry deposition across North America. *Environ. Sci. Technol.* 50, 12864–12873.